AJEMA GLOBAL RESEARCH NETWORK

AMERICAN Journal of Engineering, Mechanics and Architecture
Volume 2, Issue 4, 2024 ISSN (E): 2993-2637

Comparative Analysis of Free and Forced Convection for Aluminum and Copper-Made Radiator Tube

Gandhi M
Department of Mechanical Engineering,
Dhaanish Ahmed College of Engineering, Chennai, Tamil Nadu, India.
gandhi@dhaanishcollege.in

Manikandan S
Department of Mechanical Engineering,
Dhaanish Ahmed College of Engineering, Chennai, Tamil Nadu, India.
manikandan@dhaanishcollege.in

B. Vaidianathan
Department of Electronics & Communication Engineering
Dhaanish Ahmed College of Engineering, Chennai, Tamil Nadu, India.
vaidianathan@dhaanish college.in

Abstract: When it comes to mechanical characteristics, banana fibre is second to none, and it's abundant in nature. Efficient cooling can extend the life of the engine and enhance its performance. In order to evaluate the relative heat dissipation capabilities of aluminium and copper radiator tubes, this project calls for the construction of a flow heat exchanger. We calculated heat transfer and total efficiency using the log mean temperature difference approach. The ANSYS software was also used for the thermal behaviour investigation. A cooling fan is important to this project's simulation of real-time conditions for moving and idle variables (forced and free convection). Both theoretical and experimental investigations into cross-flow heat exchangers have yielded the following results: the heat transfer and overall heat transfer coefficients are determined by using the log mean temperature difference method, which is dependent on the inlet and outlet fluid temperatures as well as the effectiveness of the device. This finding demonstrates that heat transfer is linearly proportional to the mass flow rate of air and that its effectiveness is inversely proportional to the mass flow rate.

Keywords: Ansys Fluent; Convection Heat Transfer; Heat Exchanger; Engine Oil SAE 5w30; Anemometer; Speed Control Regulator

Introduction

The internal combustion engines found in modern automobiles produce an enormous quantity of thermal energy. The combustion chamber is responsible for producing this heat by lighting the fuel and air combination [6]. The internal combustion engine generates thrust by the explosion of the piston, which in turn turns the crankshaft by pulling on the connecting rods [7-13]. In the vicinity of the combustion chamber, metals can reach temperatures higher than 1000°F. Efficient heat disposal is

essential to avoid engine oil, cylinder walls, pistons, valves, and other components from being overheated by these extremely high temperatures. The mechanical work consumes 25% of the heat, the exhaust gases lose 35%, and the lubrication system loses 5%. At least 35% of the heat should be dissipated by the cooling system [15-19].

In favour of the more efficient liquid-cooled system, automotive engines have abandoned the air-cooled one [20]. A heat-absorbing coolant runs throughout the engine in a liquid-cooled system, particularly in the cylinder head area of the engine block, to dissipate heat, particularly around the combustion chamber. After soaking up the heat from combustion, the coolant is pushed back out into the atmosphere via the radiator after going through the engine. After cooling, the liquid is transported to the engine for recirculation [21-25]. Heat exchangers can be found in many different types of machinery and appliances, including: boilers, condensers, evaporators, regenerators, oil coolers for heat engines, milk chillers in pasteurising facilities, radiators in automobiles, and many more industrial operations [26]. When the intake and outlet conditions are determined, the logarithmic mean temperature difference (LMTD) can be used to build heat exchangers. To simplify the analysis of finding the inlet or exit temperature of a specific heat exchanger, one can use a method that relies on the heat exchanger's effectiveness (a concept initially put forward by Nusselt) and the number of transfer units (NTU). The effectiveness of a heat exchanger is defined as the ratio of its actual heat transfer to its maximum possible heat transfer [27-33].

An apparatus that allows the transfer of thermal energy between fluids of various temperatures is known as a heat exchanger. The flow of coolant through the tube and the airflow over the fins. The two fluids are kept separate as they flow at right angles to one another. As a result, heat is transferred from the coolant to the air. In cross-flow heat exchangers, this flow is used [34-41]. The term "cross-flow heat exchanger" refers to a piece of machinery that allows heat to be transferred between fluids of different temperatures [42]. Typically, in a cross-flow heat exchanger, the two streams of fluid travel in opposite directions. Improving the number of turns in a cross-flow heat exchanger decreases the oil flow rate while increasing the heat transfer (Figure 1).

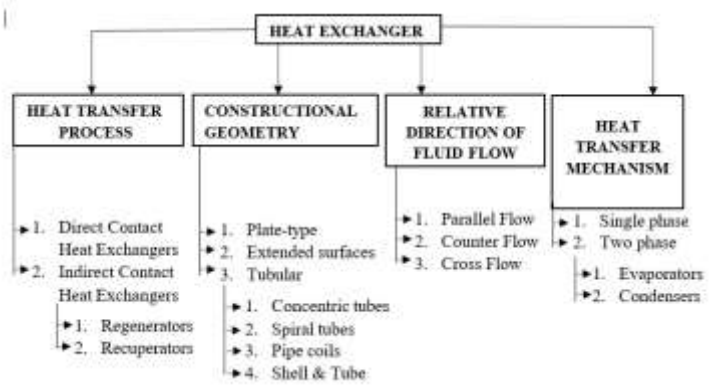

Figure 1: Classification of heat exchanger

The two fluid streams, one hot and one cold, move through the heat exchanger in the same direction in a parallel flow heat exchanger. One end of the heat exchanger receives the fluid streams, while the other end is where they exit [43-49]. It is evident from the heat exchanger's schematic and temperature profile that the fluid streams' temperature difference reduces as it moves from the entrance to the outlet of the parallel flow heat exchanger (Figure 2).

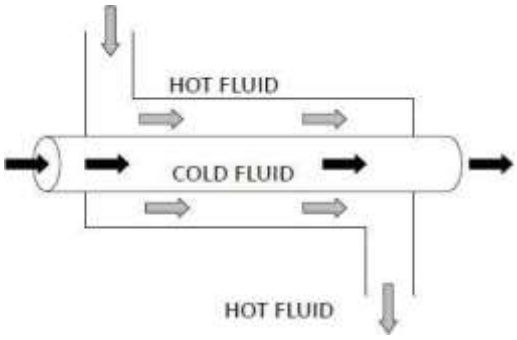

Figure 2: Parallel flow heat exchanger

The two fluid streams, one hot and one cold, move in nearly opposite directions in a heat exchanger known as a counterflow. The two streams of fluid meet at opposing points. The disparity in temperature between the two streams of fluid is very stable [50-55]. The maximum heat transfer rate for a specific surface area can be found using counterflow heat exchangers (Figure 3).

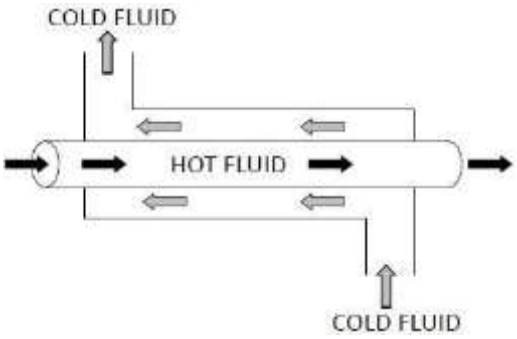

Figure 3: Counter flow heat exchanger

Typically, in a cross-flow heat exchanger, the two streams of fluid travel in opposite directions. The cross-flow heat exchanger is depicted schematically. Air is utilised as the cooling media in our laboratory's finned type cross-flow heat exchanger (Figure 4).

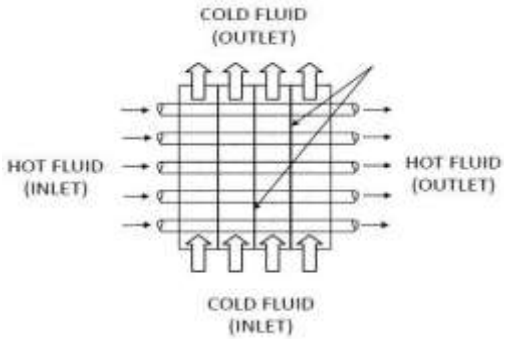

Figure 4: Cross-flow heat exchanger

The shell of this heat exchanger is typically cylindrical, and it encases a bundle of tubes. The orientation of the tubes is parallel to the axis of the shell. The tubes form a bundle, and one stream of fluid travels through them, while the other runs across the shell [56-60]. By utilising numerous shell & tube passes with baffles, the heat transmission between the fluid streams is improved. The fluid stream on the shell

side is redirected to flow in a reciprocating fashion over the tubes.

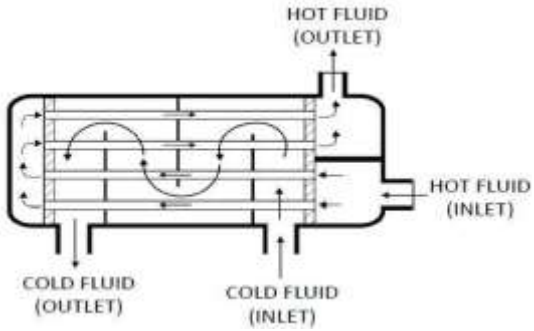

Figure 5: Shell & Tube heat exchanger

Plate heat exchangers are made up of a series of interconnected thin metal plates that have been corrugated (Figure 5). The fluid streams are distributed to the plates after entering the heat exchanger through the frame connections. Between each set of plates, there is a space that the two fluid streams flow through in opposite directions. Overall, the heat transfer between the fluid streams is improved because the metal plate grooves and tiny spacing create a turbulent flow [61-66]. Additionally, the flow's eddies clean the heat exchanger's surface, reducing fouling. Plate heat exchangers are widely used in industries due to their low cost, easy maintenance, and high thermal efficiency (Figure 6).

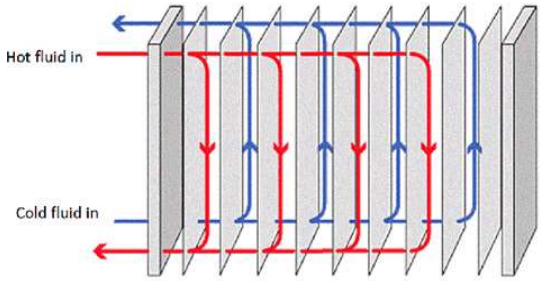

Figure 6: Plate-type heat exchange

To describe the application of infinitesimally "differential elements" in calculus and partial differential equations, the phrase "finite element" is used. Accurately determining values from analyses might be challenging, however this method helps with complicated structure analysis [67-81]. A more refined approach to conducting in-depth analyses of stresses, displacements, and support reactions in complicated shapes is made possible by increasing the number of small elements in MESH rather than the number of larger ones. This, in turn, produces more accurate conclusions. After 40 years, FEA has expanded its scope to include more complicated boundaries than finite differential equations [82]. When an agent specifies a software artefact to achieve goals with a collection of basic components that are subject to limitations, this is called software design. To design software is to engage in "all the work involved in envisioning, framing, implementing, commissioning, and eventually altering complex systems" or "the activity following requirements definition and preceding programming, as in a stylized software engineering process." Designing software typically entails figuring out problems and making plans for software solutions. Everything from low-level components to high-level architecture design and algorithm design falls under this category [83-89].

Literature Review

Radiators in cars use a circular heat exchanger, which Chavan and Tasgaonkar [1] describe. Because the air drawn in by the fan condenses into a small, circular region, the radiator's corners tend to get

very hot, necessitating a redesign of the heat exchanger to a more rectangular or square form. In the current layout, the power consumption of the fan is minimised because there is no heat transfer area in the centre, where the airflow is practically nonexistent. Create a round radiator with no corners for maximum efficiency.

The prismatic cells, also known as Li-ion cells, are addressed by Mayer et al. [2], who divide them into two cooled modules at the base. The top module incorporates a channel into its structure, while the bottom module makes use of cooling fins. Cylindrical cells are exposed to ambient air through the process of airflow via openings in the lateral cell surfaces. The fin allows heat to be transmitted from the battery pack to the air, and vice versa. Due to the fact that the extra weight of the fins exceeds the cooling benefits, using them to cool the electric car battery has become less popular.

The incorporation of fins was the primary emphasis of Kavitha et al. [3] in their investigation into methods to enhance and accelerate the cooling rate of radiators. Raising the contact surface area is the guiding idea of this approach. Altering the present fin geometry or creating new ones can enhance the contact surface, which in turn improves the heat dissipation rate. Radiators with broad contact surfaces, such as round fins, exhibit the highest temperature decrease compared to those with sharp or box fins, and the use of nanofluids as a coolant further enhances this heat dissipation. Improved convection between the nanoparticles and the surfaces of the base liquid gives it a high thermal conductivity.

The electronic controller for the cooling system was developed by Fatouh et al. [4]. The engine coolant temperature is controlled by the coolant flow rate and the speed of the radiator fan. The controller for the cooling system takes into account both linear quadratic regulation (LQR) and proportional integral derivative (PID) methods of control. The temperature of the engine's coolant can be adjusted using either the flow rate of coolant or the speed of the radiator fan. Depending on the engine load under various operating situations, to provide command control signals for the electric water pump and electric radiator fan.

In order to characterise the performance of the heat exchanger and to evaluate the present state of temperature control, Jignesh and Chaudhari [5] describe the cross-flow heat exchanger experiment setup as a helpful tool for analysing various parameters of finned tube heat exchangers and for testing heat loss. In general, a finned tube heat exchanger allows for faster heat transfer rates than one without one.

Problem Identification

- High thermal stress and decreased engine efficiency result from insufficient heat removal from the engine.
- It isn't the best cooling solution because it won't work in temperatures higher than 60 degrees Celsius.
- Keep the cooling fan and pump running as little as possible.
- Air contact surface decreases as contact surface area increases, resulting in subpar cooling.
- Make the radiator's block core larger.
- Tubes bent into a round profile.
- The astronomically priced circular radiators require the production of dies.

Research Gap

Many recent developments and investigations in engineering have focused on heat exchangers. A major breakthrough in engineering is also brought about by the analysis. As a result, we will be comparing heat exchangers manufactured of aluminium and copper using free and forced convection in our research. In order to find the heat transfer and total heat transfer coefficients, the log mean temperature difference (LMTD) approach was chosen. Compare the projected effectiveness from the NTU approach with the experimentally determined heat exchanger effectiveness [90-95]. However, no one has yet used finite element analysis to examine the materials. Now that we have done extensive research and study on the material, we can use finite element analysis to determine its mechanical and thermal properties (Figure 7).

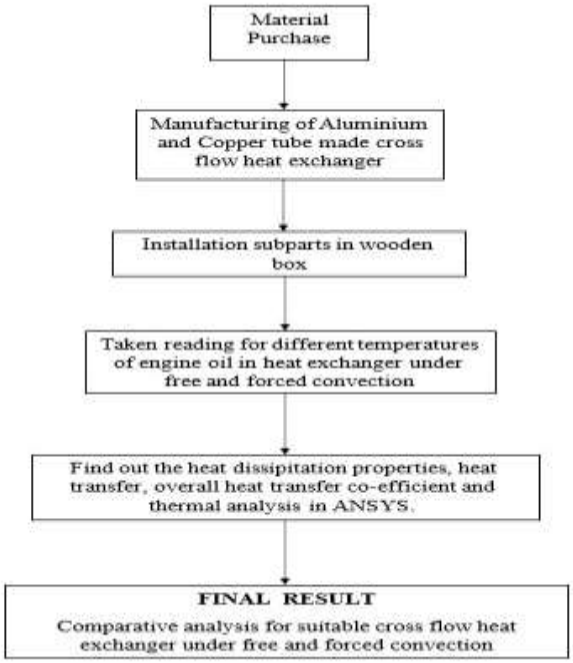

Figure 7: Fabrication process flow diagram

Mathematical Equations of Cross-Flow Heat Exchanger

There are two different method to determine the free and forced convection for aluminium and copper made heat exchanger.

- **FORCED CONVECTION:**

Heat transfer surface area, A = 0.03749 m^2

Cross-section area of the air inlet, Ac = 0.0319 m^2

Log mean temperature difference method:

the heat transfer between two fluids can be calculated from:

For Heat Transfer: $Q = F_T U A \Delta T_{lm}$

For heat transfer co-efficient:

Bulk mean temperature $T_m = \frac{T_{mi} + T_{mo}}{2}$

Reynolds number: $Re = \frac{UD}{\gamma}$

Nusselt number: $Nu = \frac{hD}{k}$

Log mean temperature difference method:

$$(\Delta T)_m = \frac{(T_1 - t_2) - (T_2 - t_1)}{\ln \frac{(T_1 - t_2)}{(T_2 - t_1)}}$$

Xaxis value: $P = \frac{t_2 - t_1}{T_1 - t_1}$

Curve value R: $R = \frac{T_1 - T_2}{t_2 - t_1}$

Effectiveness-NTU Method

The effectiveness can be calculated form equation

Effectiveness of heat exchanger:

$$\epsilon = \frac{T_1 - T_2}{T_1 - t_1}$$

Capacity rate of Engine oil (Hot fluid):

$$C_h = \dot{m}_h \times C_{ph}$$

Capacity rate of Air (Cold fluid): $C_c = \dot{m}_c C_{pc}$

Curve $\frac{C_{min}}{C_{max}}$

Number of Transfer Units: $NTU = \frac{UA}{C_{min}}$

- **FREE CONVECTION:**

the heat transfer between two fluids can be calculated from: For

Heat Transfer: $Q = hA\Delta T = hA(T_w - T_\infty)$

Film Temperature: $T_f = \frac{T_w + T_\infty}{2}$

$$\beta = \frac{1}{T_{f\,in\,K}}$$

Experimental Work

The thermal engineering laboratory of heat transfer in the mechanical engineering department of Dhaanish Ahmed College of Engineering designed and manufactured the cross-flow heat exchanger (Table 1).

Table 1: Reading of Copper radiator under Forced convection

No. of iteration	Engine oil inlet	Engine oil outlet	Air inlet	Air outlet	Mass flow rate	Engine oil flow velocity	Airflow
	in °C	in °C	in °C	in °C	in Kg/s	in m/s	in m/s
1	50	35.7	26.7	28.3	7.5×10^{-3}	0.137	5
2	71	56.9	28.14	30.4	0.0106	0.195	10
3	100	77.5	30.2	32.9	0.0136	0.256	15
4	125	109.7	31.4	33.8	0.01537	0.295	22

Heat transfer surface area, A = 0.03749 m^2
The cross-section area of the air inlet, Ac = 0.0319 m^2

To determine and verify the experimental heat transfer and engine oil temperature at the output, we have chosen to use a log mean temperature difference approach (Figure 8).

We know that, T_1=50°C, T_2=35.7°C, t1= 26.7°C,t2=28.3°C

Bulk mean temperature, $T_m = \frac{T_1+T_2}{2}$

$$T_m = \frac{50 + 35.7}{2} = 42.85°C$$

ρ=867.725kg/m^3, γ=7.77×$10^{-3}$$m^2$/s, k=0.1565W/$m^2$k, Cp=2.346×$10^3$ J/kgk

Reynolds number: $Re = \frac{UD}{\gamma} = .137\times9\times10^{-3}/7.77\times10^{-5} = 15.85$

Since Re<2300, Flow is laminar.

For laminar flow, Nusselt number, Nu=3.66

The Xaxis value is 0.06, and the curve value is 8.9375, the corresponding Y_{axis} value is 0.98,
F = 0.98

Effectiveness-NTU Method

The effectiveness can be calculated form equation

Effectiveness of heat exchanger:

$$\epsilon = \frac{T_1-T_2}{T_1-t_1} = \frac{50-35.7}{50-26.7} = 0.536$$

(From HMT data book Page No. 161 (Ninth Edition)

Capacity rate of Engine oil (Hot fluid):

$C_h = \dot{m}h \times Cph$

$= 7.548\times10^{-3}\times2.546\times10^3 = 17.707 W/k$

Capacity rate of Air (Cold fluid): $C_c = \dot{m}_c C_{pc}$

$= 0.1768\times1.007\times10^3 = 178.0376 W/k$

C_{min} = 17.707W/k, C_{max} = 178.0376W/k

(To find NTU, refer HMT data book Page No. 174 (cross flow)

From graph, $Y_{axis} = \epsilon = 0.536$

$$Curve = \frac{C_{min}}{C_{max}} = \frac{17.707}{178.037} = 0.099$$

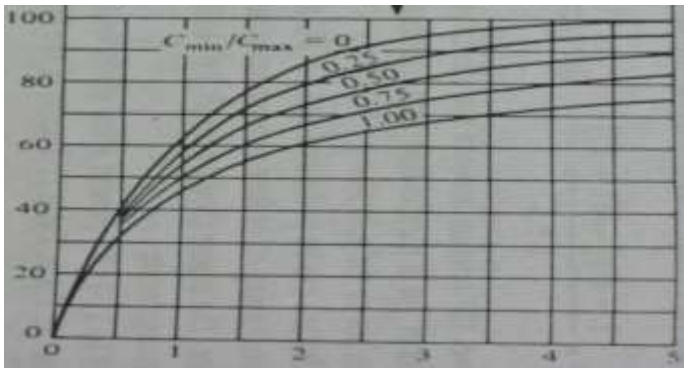

Figure 8: Effectiveness – Cross-flow, Both fluids unmixed for the copper radiator.

The corresponding Xaxis value is 0.89, NTU=0.89
Number of Transfer Units: NTU = UA
Cmin

0.89 = U×0.03749
17.707

U = 420.35W/m2k

For Heat Transfer: $Q=FTUA\Delta Tlm$ = 0.98×420.35×0.03749×14.4 = 222.389 W (Table 2).

Table 2: Reading of Aluminum radiator under Forced convection

No. of iteration	Engine oil inlet	Engine oil outlet	Air inlet	Air outlet	Mass flow rate	Engine oil flow velocity	Airflow
	in °C	in °C	in °C	in °C	in Kg/s	in m/s	in m/s
1	50	42.9	27.1	29.5	5.83×10^{-3}	0.134	5
2	71	64.3	29.3	30.9	9.114×10^{-3}	0.213	10
3	100	81.4	28.9	29.7	0.0123	0.294	15
4	125	116.8	30.1	32.3	0.0148	0.359	22

Heat transfer surface area, A = 0.04824 m^2
The cross-section area of the air inlet, Ac = 0.0423 m^2

In order to determine and verify the experimental heat transfer and engine oil temperature at the outlet, the log mean temperature difference approach has been chosen:

Iteration1:

We know that, T_1=50°C, T_2=42.9°C, t1= 27.1°C, t2=29.5°C

Bulk mean temperature, $T_m = \frac{T_1+T_2}{2}$

$$T_m = \frac{50 + 42.9}{2} = 46.45°C$$

Properties of Engine oil at 46.45°C:

(From HMT data book Page No. 33 (Ninth Edition)

ρ=866.15kg/m^3, **γ**=6.97×$10^{-5}$$m^2$/s, k=0.155W/$m^2$k, Cp=2.297×$10^3$J/Kgk

Reynolds number: $Re = \frac{UD}{\gamma} = .134\times9\times10^{-3}/6.97\times10^{-5} = 15.36$

Since Re<2300, Flow is laminar.

For laminar flow, Nusselt number, Nu=3.66

(From HMT data book Page No. 132 (Ninth Edition)

Nusselt number: $Nu = \frac{hD}{k}$

$3.66=h\times9\times10^{-3}/0.155$

Heat transfer Co-efficient, h=70.91W/m^2k.

This is cross flow, both fluids unmixed type heat exchanger

$$Q=F_T U A \Delta T_{lm}$$

(From HMT data book Page No. 160 (Ninth Edition)

Log mean temperature difference method:

$$(\Delta T)_m = \frac{(T_1-t_2)-(T_2-t_1)}{\ln\frac{(T_1-t_2)}{(T_2-t_1)}} = \frac{(50-29.5)-(42.9-27.1)}{\ln\frac{(50-29.5)}{(42.9-27.1)}} = 18.04°C$$

Page 170 of the HMT data book (Ninth Edition) (Single-pass cross flow heat exchanger - Both fluids unmixed) contains the correction factor F.

In order to resolve the analysis, we employ ANSYS 15. We begin by using the precise model dimensions to create the 3D geometry in Solidworks 13. Then, we proceed to add material data for the cross-flow heat exchanger made of aluminium and copper one by one. By utilising SOLIDWORKS, the precise proportions of the heat exchanger may be modelled by repurposing existing materials [96-101]. Before being imported into Ansys Fluent for thermal analysis, the modelled cross-flow tubes and fins are built in Solidworks (Figures 9 and 10).

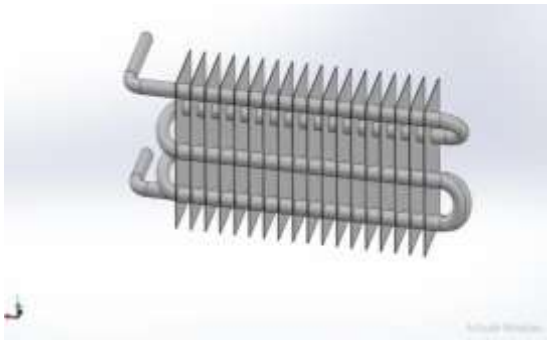

Figure 9: Copper tube radiator

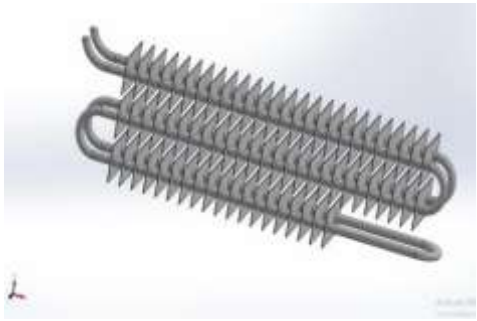

Figure 10: Aluminum tube radiator

The Finite Element Method, a numerical approach, is used in Finite Element Analysis (FEA), which simulates any physical process (FEM). An assembly's or part's behaviour under specified conditions can be predicted using finite element analysis (FEA). Modern simulation software is based on it, and engineers utilise it to uncover design weaknesses, tension points, and other issues. A colour scale that illustrates the distribution of pressure and temperature around the object, for example, is a common way to represent the results of FEA-based simulations. This study examines and presents the methods that was utilised to design the heat exchanger. As a result of

As part of the design process, the pressure drops, surface area for heat transfer, and cross-flow and tube-side heat transfer coefficients must be determined. In order to assess the part's rigidity under design pressures, the mechanical design of the heat exchanger incorporates calculations of the part's thickness, including the cross-flow channel, tube, and so on [102-107]. The thermal analysis behaviour of heat exchangers constructed of copper and aluminium is investigated in the ANSYS simulation by means of repetitive cooling system applications. Vehicle dynamics are required to ascertain the temperature variation with respect to vehicle speed. On the other hand, this research contrasted the results of free and forced convection analyses for radiator tubes constructed of aluminium and copper. After that, we use ANSYS to study the heat exchanger model that we created in Pro-Engineer. Here, oil is considered the hot fluid and air, the cold fluid, as none of these states undergoes phase change. As the coolant velocity increases, so does the heat transfer coefficient and the pressure drop. As the fluid's velocity increases, the thickness of the temperature boundary layer on the tube decreases [108-111]. A clear picture of the three-dimensional fluid flow can be obtained from flow trajectories, which display the flow streamlines.

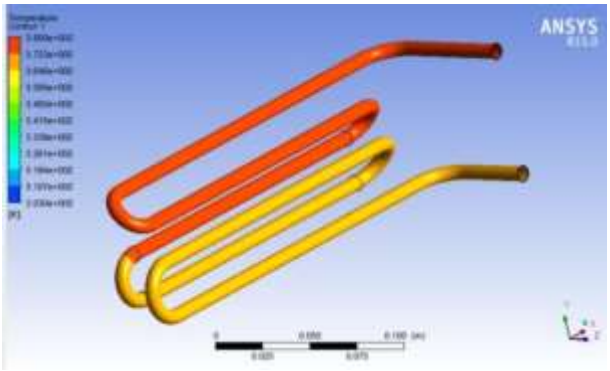

Figure 11: Heat transfer in copper

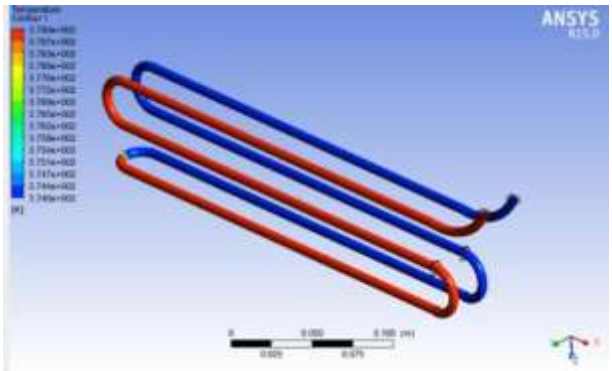

Figure 12: Heat transfer in aluminum Radiator

Radiator

The coolant flow temperatures at the intake and exit of the copper tube radiator are 380°K and 356.9°K, respectively, as shown in Figure 11. In the aluminium tube radiator, the corresponding temperatures are 379°K and 374°K, respectively, as shown in Figure 12.

Result and Discussion

The two fluids are kept separate as they flow at right angles to one another. As a result, heat is transferred from the coolant to the air. In cross-flow heat exchangers, this flow is used. As the coolant velocity increases, so does the heat transfer coefficient and the pressure drop. As the fluid's velocity increases, the thickness of the temperature boundary layer on the tube decreases. A clear picture of the three-dimensional fluid flow can be obtained from flow trajectories, which display the flow streamlines (Table 3).

Table 3: Results of Experimental Work in Copper and Aluminum Radiator

Description	**Mate Real of Flow Tube**		**Results**			
		Iteration	**Heat Transfer Coefficient in W/m^2K**	**Overall Heat Transfer Coefficient in W/m^2K**	**Heat Trans Fer Rate in Watts**	**Effectiveness**
Forced Convection	Copper	1	63.643	420.35	222.38	0.536
		2	60.59	301.436	380.65	0.328
		3	58.96	290.04	616.71	0.322
		4	57.34	280.22	907.09	0.16
	Aluminium	1	70.91	111.026	93.72	0.31
		2	67.02	104.75	185.84	0.26
		3	66.33	95.5	276.58	0.1616
		4	64.5	90.3217	386.36	0.086
Free Convection	Copper	1	63.44	406.812	218.06	0.545
		2	60.59	307.64	310.65	0.285
		3	58.96	294.1337	661.24	0.262
		4	57.34	239.178	789.02	0.124
		1	70.22	87.6	78.54	0.227
	Aluminum	2	67.893	104.97	193.02	0.215
		3	45.04	140.67	425.29	0.203
		4	42.15	144.145	638.72	0.0518

Moreover, that occurred because an increase in velocity causes a rise in the Reynolds number, which in turn increases the quantity of air that comes into contact with the surface of the heat exchanger in order to lower the temperature. When Q=907.09Watma=0.6288kg/s, the maximum heat transfer occurs.

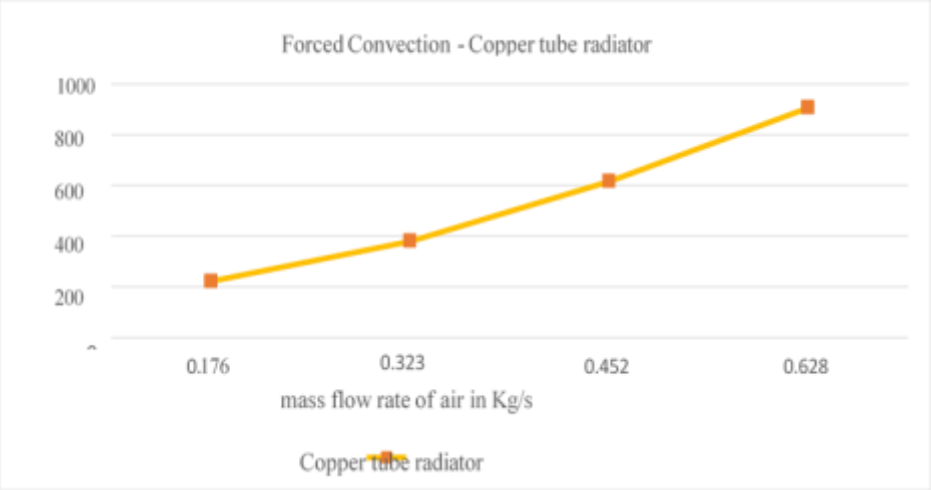

Figure 13: Relationship between heat transfer and mass flow rate of air with forced convection for Copper radiator

Figure 13 demonstrates that when the mass flow rate of air rose, heat transfer increased, when the engine oil flow rate is 5.83×10-3Kg/s at Q=93.72 W. Moreover, that occurred because an increase in velocity causes a rise in the Reynolds number, which in turn increases the quantity of air that comes into contact with the surface of the heat exchanger in order to lower the temperature. P=0.833 kg/s yields a maximum heat transfer of Q=386.36 W.

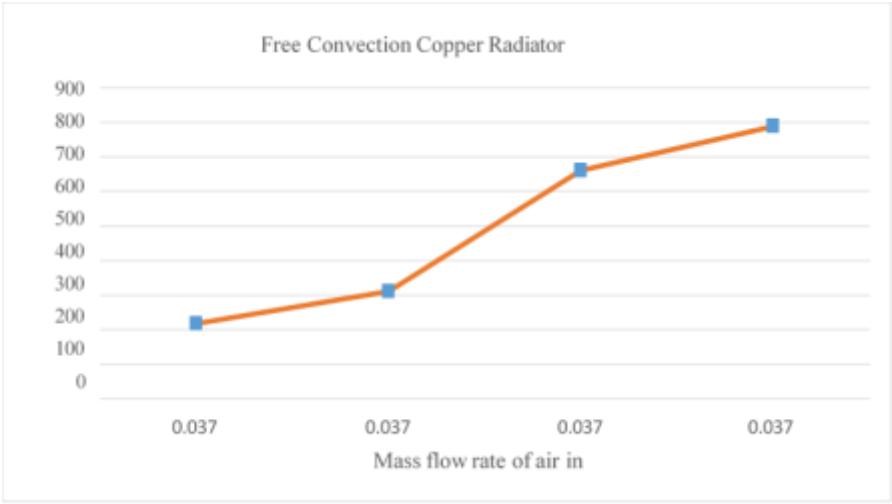

Figure 14: Relationship between heat transfer and mass flow rate of air with forced convection for Aluminum radiator

The heat transfer increased as the mass flow rate of air rose, as shown in Figure 14, when the engine oil flow rate is 7.4×10-3Kg/s and Q=218.06 W. Moreover, that occurred because an increase in velocity causes a rise in the Reynolds number, which in turn increases the quantity of air that comes into contact with the surface of the heat exchanger in order to lower the temperature. At mass flow rate of 0.0377 kg/s, the maximum heat transfer is Q=789.024 W.

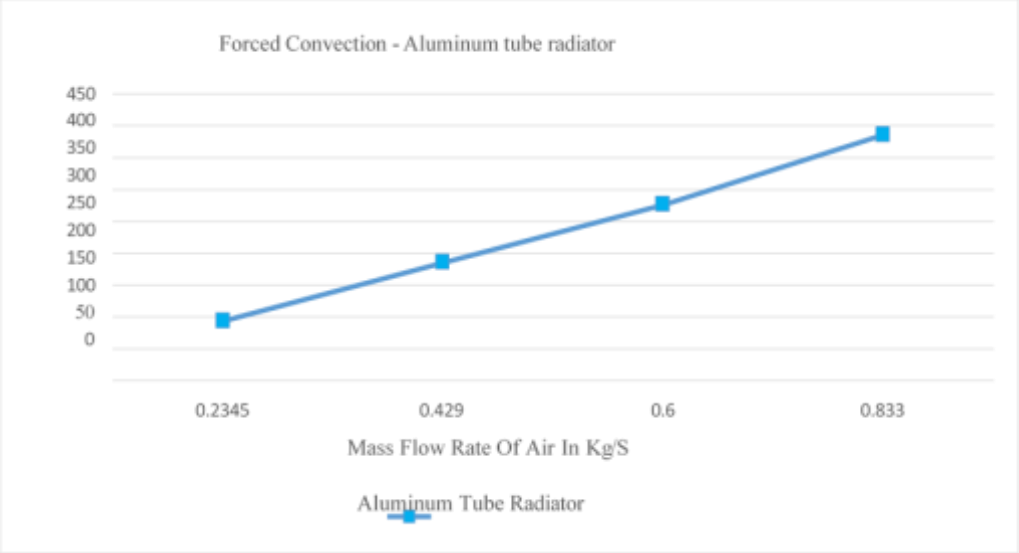

Figure 15: Relationship between heat transfer and mass flow rate of air with free convection for Copper radiator

A higher mass flow rate of air resulted in an increase in heat transfer, as seen in Figure 15, when the engine oil flow rate was 6.16×10-3Kg/s and Q=78.54 W. Moreover, that occurred because an increase in velocity causes a rise in the Reynolds number, which in turn increases the quantity of air that comes into contact with the surface of the heat exchanger in order to lower the temperature. When ma=0.05 kg/s, the maximum heat transfer is 638.72 W.

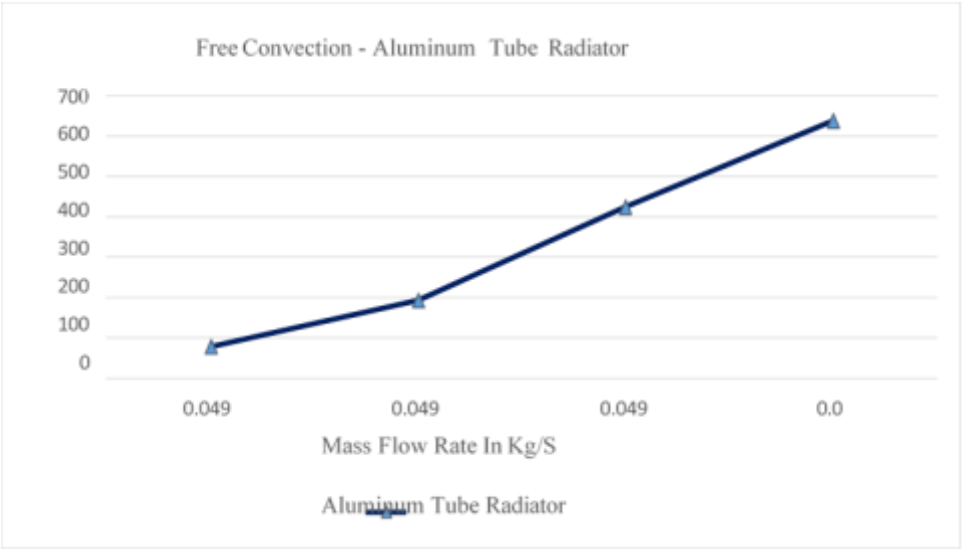

Figure 16: Relationship between heat transfer and mass flow rate of air with free convection for Aluminum radiator

As seen in Figure 16, the efficiency behaviour during the transfer of air mass is illustrated. The efficiency drops as the air mass flow rate rises, and Assuming an airflow rate (ma) of 0.1768 kg/s, the minimum efficacy is determined to be 53.6%. Because, depending on the effectiveness connection, the

mass flow rate of air is inversely related to the effectiveness, that is what transpired. When the airflow rate (ma) was 0.6288 kg/s, the minimum effectiveness was 16 percent.

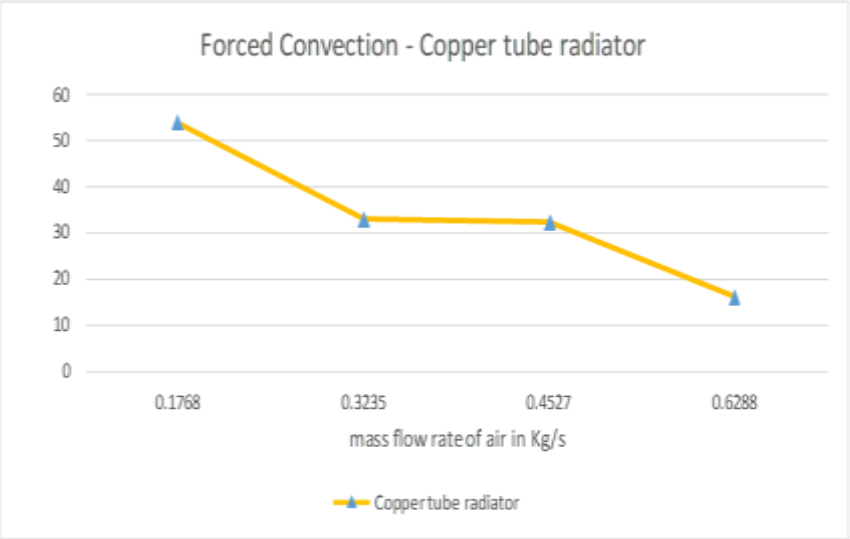

Figure 17: Relationship between effectiveness and mass flow rate with forced convection For Copper radiator

We used forced convection to build a copper tube cross-flow heat exchanger in a two-wheeler vehicle so that we could regulate the temperature of the engine oil and keep the protective film of lubricating oil from degrading and losing its lubricating capabilities (Figure 17). Heat exchangers can be found in many different types of machinery and appliances, including: boilers, condensers, evaporators, regenerators, oil coolers for heat engines, milk chillers in pasteurising facilities, radiators in automobiles, and many more industrial operations.

Conclusion

We find that the heat transfer rate is high when the copper tube radiator is subjected to forced convection, as shown by comparing the graphs obtained from the analysis with the free convection findings. The heat exchanger's efficiency in free convection with a copper tube radiator is improved by keeping an eye on the results of the thermal study. The structural analysis shows that heat exchangers operating under free convection have better heat dissipation characteristics than those operating under forced convection. The heat transfer and total heat transfer coefficients have been calculated using the log mean temperature difference approach, which is effective with respect to the fluid's inlet and outlet temperatures. Increasing the mass flow rate of air in structural analysis enhances heat transmission, as shown by this conclusion. More so, the efficacy diminishes as the air mass flow rate rises. In order to determine the rate of heat transfer, this study will compare and contrast current radiators. An Arduino screen, which shows the results of the tests on your computer, is a great addition to the lab. Consider utilising other heat exchangers. Gaining an understanding of the cooling engines you'll need, as well as the heat exchanger's efficiency and cooling capacity, is within your reach with this project.

References

1. D. Chavan and G. S. K Tasgaonkar, "Analysis And Design Of Automobile Radiator (Heat Exchanger) Proposed With Cad Drawings And Geometrical Model Of The Fan," Analysis And Design Of Automobile Radiator (Heat Exchanger) Proposed With Cad Drawings And Geometrical Model Of The Fan", vol. 3, pp. 137–146, 2013.
2. B. Mayer, M. Schier, and H. E. Friedrich, "Stand-alone battery thermal management for fast charging of electric two wheelers integrated busbar cooling," World Electric Veh. J., vol. 10, no. 2, p. 37, 2019.
3. M. K. R. Kavitha et al., "Modeling of automotive radiator by varying structure of fin and coolant," International Journal of Recent Technology and Engineering (IJRTE), vol. 8, no. 2, pp. 2139–2146, 2019.
4. M. Fatouh, S. El-Demerdash, M. Mohamed, and M. H. Shedid, "Performance of electronically controlled automotive engine cooling system using PID and LQR control techniques" IOSR Journal of Mechanical and Civil Engineering" vol. 08, no.3, pp. 42–51, 2018.
5. M. Jignesh and D. Chaudhari, "Experimental Investigation of Finned Tube Heat Exchanger," International Journal of Innovative Research in Advanced Engineering, vol. 01, no. 5, pp. 67–73, 2014.
6. O. Fabela, S. Patil, S. Chintamani, and B. H. Dennis, "Estimation of effective thermal conductivity of porous media utilizing inverse heat transfer analysis on cylindrical configuration," in Volume 8: Heat Transfer and Thermal Engineering, 2017.
7. S. Patil, S. Chintamani, B. H. Dennis, and R. Kumar, "Real time prediction of internal temperature of heat generating bodies using neural network," Therm. Sci. Eng. Prog., vol. 23, no. 100910, p. 100910, 2021.
8. S. Patil, S. Chintamani, J. Grisham, R. Kumar, and B. H. Dennis, "Inverse determination of temperature distribution in partially cooled heat generating cylinder," in Volume 8B: Heat Transfer and Thermal Engineering, 2015.
9. P. Paramasivan, "A Novel Approach: Hydrothermal Method of Fine Stabilized Superparamagnetics of Cobalt Ferrite (CoFe2O4) Nanoparticles," Journal of Superconductivity and Novel Magnetism, vol. 29, pp. 2805–2811, 2016.
10. P. Paramasivan, "Controllable synthesis of CuFe2O4 nanostructures through simple hydrothermal method in the presence of thioglycolic acid," Physica E: Low-dimensional Systems and Nanostructures, vol. 84, pp. 258–262, 2016.
11. S. Ambika, T. A. Sivakumar, and P. Sukantha, "Preparation and characterization of nanocopper ferrite and its green catalytic activity in alcohol oxidation reaction," Journal of Superconductivity and Novel Magnetism, vol. 32, pp. 903–910, 2019.
12. P. Paramasivan, "Comparative investigation of NiFe2O4 nano and microstructures for structural, optical, magnetic and catalytic properties," Advanced Science, Engineering and Medicine, vol. 8, pp. 392–397, 2016.
13. P. Paramasivan, S. Narayanan, and N. M. Faizee, "Enhancing Catalytic Activity of Mn3O4 by Selective Liquid Phase Oxidation of Benzyl Alcohol," Advanced Science, Engineering and Medicine, vol. 10, pp. 1–5, 2018.
14. D. Balasubramaniam, H. P. Nguyen, P. Q. H. Le, V. V. Pham, X. P. Nguyen, et al., "Application of the Internet of Things in 3E (efficiency, economy, and environment) factor-based energy management as smart and sustainable strategy," Energy Sources, Part A: Recovery, Utilization, and Environmental Effects, pp. 1–23, 2021.
15. W.-H. Chen, A. T. Hoang, S. Nižetić, A. Pandey, C. K. Cheng, et al., "Biomass-derived biochar:

From production to application in removing heavy metal-contaminated water," Process Safety and Environmental Protection, vol. 160, pp. 704–733, Apr. 2022.
16. M. M. Noor, X. D. Pham, and A. T. Hoang, "Comparative analysis on performance and emission characteristic of diesel engine fueled with heated coconut oil and diesel fuel," International Journal of Automotive and Mechanical Engineering, vol. 15, no. 1, pp. 5110–5125, 2018.
17. N. Kaur and S. D. Tiwari, "Role of particle size distribution and magnetic anisotropy on magnetization of antiferromagnetic nanoparticles," J. Phys. Chem. Solids, vol. 123, pp. 279–283, 2018.
18. N. Kaur and S. D. Tiwari, "Thermal decomposition of ferritin core," Appl. Phys. A Mater. Sci. Process., vol. 125, no. 11, 2019.
19. N. Kaur and S. D. Tiwari, "Role of wide particle size distribution on magnetization," Appl. Phys. A Mater. Sci. Process., vol. 126, no. 5, 2020.
20. N. Kaur and S. D. Tiwari, "Evidence for spin-glass freezing in NiO nanoparticles by critical dynamic scaling," J. Supercond. Nov. Magn., vol. 34, no. 5, pp. 1545–1549, 2021.
21. N. Kaur and S. D. Tiwari, "Estimation of magnetic anisotropy constant of magnetic nanoparticles," in DAE Solid State Physics Symposium 2019, 2020.
22. H.A.A. Alsultan and K. H. Awad "Sequence Stratigraphy of the Fatha Formation in Shaqlawa Area, Northern Iraq," Iraqi Journal of Science ,vol. 54, no.2F, p.13-21, 2021.
23. H.A.A. Alsultan , M.L. Hussein, , M.R.A. Al-Owaidi , A.J. Al-Khafaji and M.A. Menshed "Sequence Stratigraphy and Sedimentary Environment of the Shiranish Formation, Duhok region, Northern Iraq", Iraqi Journal of Science, vol.63, no.11, p.4861-4871, 2022.
24. H.A.A. Alsultan , F.H.H. Maziqa and M.R.A. Al-Owaidi "A stratigraphic analysis of the Khasib, Tanuma and Sa'di formations in the Majnoon oil field, southern Iraq," Bulletin of the Geological Society of Malaysia, vol. 73, p.163 – 169, 2022 .
25. I.I. Mohammed, and H. A. A. Alsultan "Facies Analysis and Depositional Environments of the Nahr Umr Formation in Rumaila Oil Field, Southern Iraq," Iraqi Geological Journal, vol.55, no.2A, p.79-92, 2022.
26. I.I. Mohammed, and H. A. A. Alsultan "Stratigraphy Analysis of the Nahr Umr Formation in Zubair oil field, Southern Iraq," Iraqi Journal of Science, vol. 64, no. 6, p. 2899-2912, 2023.
27. Praveen Barmavatu, Mihir Kumar Das, Rathod Subhash, Banoth Sravanthi, Radhamanohar Aepuru, R Venkat reddy, Yalagandala akshay kumar "Designing an Effective Plate Fin Heat Exchanger and Prediction of Thermal Performance Operated Under Different Water Blends Using Machine Learning", Journal of Thermal Sciences and Engineering Applications, ASME Publications, Vol-15/issue-4/pp: 041001-041022, 2023.
28. Praveen Barmavatu, S A Deshmukh, Mihir Kumar Das, Radhamanohar Aepuru, R Venkat reddy, Banoth Sravanthi "Synthesis and experimental investigation of glass fiber epoxy/saw dust composites for flexural & tensile strength", Materiale Plastice, vol-59/issue-02/pp:73-81/June 2022.
29. U.B. Vishwanatha, Y. Dharmendar Reddy, Praveen Barmavatu, B. Shankar Goud "Insights into stretching ratio and velocity slip on MHD rotating flow of Maxwell nanofluid over a stretching sheet: Semi-analytical technique OHAM", Journal of the Indian Chemical Society, Elsevier Publishers, , Vol-100/issue-3/pp: 100937-10, 2023.
30. Darapu Kiran Sagar Reddy, Praveen Barmavatu, Mihir Kumar Das, Radhamanohar Aepuru "Mechanical properties evaluation and microstructural analysis study of ceramic-coated IC engine cylinder liner", Elsevier material today proceedings, Vol-76/Part-3, pp: 518-523, 2023.
31. Darapu Kiran Sagar Reddy, Praveen Barmavatu, Mihir Kumar Das, Radhamanohar "Aepuru Experimental analysis of coated engine cylinder liners", AIP Conference Proceedings, / Vol 2786/

Paper ID: 030002, 2023.
32. Sonali Anant Deshmukh, Praveen Barmavatu, Mihir Kumar Das, Bukke Kiran Naik, Radhamanohar Aepuru "Heat Transfer Analysis in Liquid Jet Impingement for Graphene/Water Nano Fluid", Springer Lecture Notes in Mechanical Engineering (LNME), ICETMIE-2022, pp: 1079–1090.
33. Barmavatu Praveen, Madan mohan reddy Nune, Yalagandala akshay kumar, Rathod Subhash, "Investigating the Effect of Minimum Quantity Lubrication on Surface Finish of EN 47 Steel Material", Elsevier material today proceedings, , Vol-38/Part-05, pp-32-53-3257.
34. Yalagandala akshay kumar, Shaik shafee, Barmavatu Praveen "Experimental investigation of residual stresses in a die casted alluminium fly wheel" Elsevier material today proceedings /vol19/issue-Part-02/pp: A10-A18/October2019, Impact Factor- 2.59.
35. Barmavatu Praveen & S. chakradhar Goud "fabrication of compact heat exchanger with composite alloys" International journal of innovative technology and exploring engineering, 8(6S4), 717–721.
36. Barmavatu Praveen, Yalagandala Akshay Kumar, Banoth Sravanthi, H. Ameresh "Methodological Investigation on recycling of Plastic Polymers-A Review" International journal of scientific & technological research 2277-8616/vol-9/issue-03/pp:1537-1542/march 2020.
37. Barmavatu Praveen & s chakradhar goud "CFD approach for different fluids varients in compact heat exchanger at different parametric conditions" International journal of scientific & technological research, /vol-8/issue-12/pp:2288-2296/december2019. https://www.ijstr.org/paper-references.php?ref=IJSTR-1119-24385
38. Khilji et al., "Titanium Alloy Particles Formation in Electrical Discharge Machining and Fractal Analysis," JOM 2021 742, vol. 74, no. 2, pp. 448–455, Jan. 2022.
39. Khilji, S. N. B. M. Safee, S. Pathak, C. R. Chilakamarry, A. S. B. A. Sani, and V. J. Reddy, "Facile Manufacture of Oxide-Free Cu Particles Coated with Oleic Acid by Electrical Discharge Machining," Micromachines 2022, Vol. 13, Page 969, vol. 13, no. 6, p. 969, Jun. 2022.
40. Khilji, C. R. Chilakamarry, A. N. Surendran, K. Kate, and J. Satyavolu, "Natural Fiber Composite Filaments for Additive Manufacturing: A Comprehensive Review," Sustain. 2023, Vol. 15, Page 16171, vol. 15, no. 23, p. 16171, Nov. 2023.
41. R. Chilakamarry, A. M. Mimi Sakinah, A. W. Zularism, I. A. Khilji, and S. Kumarasamy, "Glycerol Waste to Bio-Ethanol: Optimization of Fermentation Parameters by the Taguchi Method," J. Chem., vol. 2022, p. 4892992, 2022.
42. R. Chilakamarry, A. M. M. Sakinah, A. W. Zularism, I. A. Khilji, and R. Sirohi, "Bioconversion of glycerol waste to ethanol by Escherichia coli and optimisation of process parameters," Indian J. Exp. Biol., vol. 60, no. September, pp. 681–688, 2022.
43. M. Qenawy, W. Zhou, and Y. Liu, "Effects of crossflow-fed-shaped holes on the adiabatic film cooling effectiveness," International Journal of Thermal Sciences, vol. 177, p. 107578, Jul. 2022.
44. M. Qenawy, W. Zhou, D. Peng, and Y. Liu, "Investigation of Film Cooling Vortical Structures Behind a Cylindrical Hole Fed by an Internal Crossflow," Sep. 2019.
45. M. Qenawy, M. Taha, and A. H. Abdelbaky Elbatran, "Unsteady adiabatic film cooling effectiveness behind shaped holes," Case Studies in Thermal Engineering, vol. 34, p. 102005, Jun. 2022.
46. M. Qenawy, A. Hamed, W. Abdelfadeel, and S. Abdelhady, "Assessment of the Planned Expansion of Renewable Energy in Egypt," International Journal of Applied Energy Systems, vol. 0, no. 0, pp. 0–0, Apr. 2022.
47. M. Qenawy, Y. Chen, J. Wang, J. Tian, and B. Chen, "Intermittent cryogen spray cooling coupled with cold air jet for heat transfer enhancement and cryogen saving of laser dermatology," Physics

of Fluids, vol. 36, no. 2, Feb. 2024.
48. M. Qenawy, J. Wang, J. Tian, B. Li, and B. Chen, "Investigation of unsteady flow behavior of cryogen-spray coupled with cold air jet," Appl Therm Eng, vol. 235, Nov. 2023.
49. M. Qenawy, M. Taha, J. Wang, and A. H. Abdelbaky Elbatran, "Effects of hole-inlet velocity on the adiabatic film cooling effectiveness behind crossflow-fed shaped holes," Appl Therm Eng, vol. 222, Mar. 2023.
50. M. Qenawy, W. Zhou, H. Chen, H. Shao, D. Peng, and Y. Liu, "Unsteady Analysis of Adiabatic Film Cooling Effectiveness Behind a Row of Circular Holes Fed by Internal Crossflow," in Volume 5B: Heat Transfer, American Society of Mechanical Engineers, Jun. 2019.
51. M. Qenawy, Y. Chen, J. Wang, J. Tian, B. Li, and B. Chen, "Transient behavior of liquid film deposition and surface heat transfer upon cryogen-spray cooling coupled with cold air jet," Int J Heat Mass Transf, vol. 223, p. 125224, May 2024.
52. W. Zhou, M. Qenawy, H. Shao, D. Peng, X. Wen, and Y. Liu, "Turbine vane endwall film cooling with barchan-dune shaped ramp in a single-passage transonic wind tunnel," Int J Heat Mass Transf, vol. 162, Dec. 2020.
53. W. Zhou, H. Shao, M. Qenawy, D. Peng, H. Hu, and Y. Liu, "Improved Turbine Vane Endwall Film Cooling by Using Sand-Dune-Inspired Design," Journal of Thermal Science, vol. 31, no. 3, pp. 958–973, May 2022.
54. J. Tian et al., "Unstable spray pattern and cooling performance of cryogen spray coupled with cold air jet: An experimental study," Physics of Fluids, vol. 35, no. 12, Dec. 2023.
55. H. S. El-Mesery, M. Qenawy, Z. Hu, and W. G. Alshaer, "Evaluation of infrared drying for okra: Mathematical modelling, moisture diffusivity, energy activity and quality attributes," Case Studies in Thermal Engineering, vol. 50, p. 103451, Oct. 2023.
56. M. Qenawy et al., "Performance and emission of extracted biodiesel from mixed Jatropha-Castor seeds," Fuel, vol. 357, p. 130060, Feb. 2024.
57. M. Qenawy, Y. Liu, and W. Zhou, "On the unsteady behaviours of the adiabatic endwall film cooling effectiveness," IOP Conf Ser Mater Sci Eng, vol. 1172, no. 1, p. 012031, Aug. 2021.
58. M. Qenawy and S. Abdelhady, "Analytical Study of a Modified Thermal Energy Storage System for PS10 in Aswan," in The International Conference on Mathematics and Engineering Physics, May 2014, pp. 1–5.
59. Mohamed Qenawy, "Matlab Simulation of 10 MW Molten Salt Solar Power Tower Plant in Aswan," Noble International Journal of Scientific Research, vol. 1, no. 1, pp. 34–43, 2017.
60. Mohamed Qenawy, S. Abdelhady, W. Abdelfadeel, and M. Shaban, "Analytical Study of a Modified PS10 in Aswan," Int J Sci Eng Res, vol. 5, no. 9, pp. 976–983, 2014.
61. H. Chen, W. Zhou, M. Qenawy, and Y. Liu, "Experimental Study on Spatio-Temporal Variation of Double-Row Holes Film Cooling Effectiveness with Oscillating Mainstream," Sep. 2019.
62. W. Zhou, M. Qenawy, Y. Liu, X. Wen, and D. Peng, "Influence of mainstream flow oscillations on spatio-temporal variation of adiabatic film cooling effectiveness," Int J Heat Mass Transf, vol. 129, pp. 569–579, Feb. 2019.
63. M. Qenawy, L. Yuan, Y. Liu, D. Peng, X. Wen, and W. Zhou, "A Novel Single-Passage Transonic Wind Tunnel for Turbine-Vane Film Cooling," J Eng Gas Turbine Power, vol. 142, no. 7, Jul. 2020.
64. M. Qenawy, H. Chen, D. Peng, Y. Liu, and W. Zhou, "Flow Structures and Unsteady Behaviors of Film Cooling from Discrete Holes Fed by Internal Crossflow," J Turbomach, vol. 142, no. 4, Apr. 2020.
65. M. Qenawy, W. Zhou, and Y. Liu, "Effects of crossflow-fed-shaped holes on the adiabatic film cooling effectiveness," International Journal of Thermal Sciences, vol. 177, p. 107578, Jul. 2022.

66. Bayas, E., Kumar, P., & Deshmukh, K. (1869). Review of process parameter's effect on 3D printing. GIS Science Journal, 10(3), 834–845.
67. Bayas, E., Kumar, P., & Harne, M. (2023). Impact of Process Parameters on Mechanical Properties of FDM 3D-Printed Parts: A Comprehensive Review. Eur. Chem. Bull, 12(S5), 708–725.
68. Bayas, Eknath, Kumar, P., & Deshmukh, K. (2023). A comprehensive review: Process parameters impact on tensile strength of 3D printed PLA parts. International Journal of Advanced Research in Science, Communication and Technology, 3(2) 233–239.
69. E Bayas, P. (2024). Impact of Slicing Software on Geometric Correctness For FDM Additive Manufacturing. International Development Planning Review, 23(1), 704–711.
70. Ananda Shankar Hati, and T. K. Chatterjee, "Symmetrical component filter based online condition monitoring instrumentation system for mine winder motor" Measurement (Elsevier), vol. 82, pp. 284-300, 2016.
71. Prashant Kumar and Ananda Shankar Hati "Review on Machine Learning Algorithm Based Fault Detection in Induction Motors," Archives of Computational Methods in Engineering, vol: 28, pp: 1929-1940, 2021.
72. Kumar Prashant and Hati, Ananda Shankar "Convolutional Neural Network with batch normalization for fault detection in SCIM," IET Electric Power Application, vol: 15, issue: 1, pp. 39-50, 2021.
73. Kumar Prashant and Hati, Ananda Shankar "Deep Convolutional Neural Network based on adaptive gradient optimizer for fault detection in SCIM," ISA Transactions, vol: 111, pp: 350-359, 2021.
74. Prince, Hati Ananda Shankar, Chakrabarti Prasun, Abawajy Jemal Hussein and Ng Wee Keong "Development of Energy Efficient Drive for Ventilation System using Recurrent Neural Network," Neural Computing and Applications, Vol. 33, no. 14, pp. 8659-8668, 2021.
75. Prince and Hati Ananda Shankar "A Comprehensive Review of Energy-Efficiency of Ventilation System using Artificial Intelligence" Renewable and Sustainable Energy Reviews (2021), vol: 146, 2021.
76. Kumar Prashant and Hati, Ananda Shankar "Transfer Learning Based Deep CNN Model for Multiple Faults Detection in SCIM" Neural Computing and Applications (2021).
77. Prince and Hati Ananda Shankar "Temperature and Humidity Dependent MRAS Based Speed Estimation Technique for Induction Motor used in Mine Ventilation Drive" Journal of Mining Science, 2021, Vol. 57, No. 5, pp. 842–851.
78. Kumar Prashant and Hati, Ananda Shankar "Dilated Convolutional Neural Network Based Model For Bearing Faults and Broken Rotor Bar Detection in Squirrel Cage Induction Motors" Expert Systems With Applications (2022).
79. Prince and Hati Ananda Shankar "Convolutional Neural Network-Long Short Term Memory Optimization for Accurate Prediction of Airflow in a Ventilation System" Expert Systems with Applications (2022).
80. Vatsa Aniket and Hati Ananda Shankar "Depolarization Current Prediction of Transformers OPI System Affected From Detrapped Charge Using LSTM," in IEEE Transactions on Instrumentation and Measurement, vol. 71, pp. 1-11, 2022, Art no. 2511711.
81. Gorai Rahul, Hati Ananda Shankar, and Maity Tanmoy, "A new cascaded multilevel converter topology with a reduced number of components" 3rd IEEE 2017 Conference on International conference on Power, Control, Signals and Instrumentation Engineering (ICPCSI-2017), 21-22 September 2017 | IEEE, Chennai, India., pp. 539-543.
82. Kumar Prashant, Hati, Ananda Shankar, Sanjeevikumar Padmanaban, Leonowicz Zbigniew and Prasun Chakrabarti "Amalgamation of Transfer Learning and Deep Convolutional Neural

Network for Multiple Fault Detection in SCIM" 2020 IEEE International Conference on Environment and Electrical Engineering and 2020 IEEE Industrial and Commercial Power Systems Europe (EEEIC/I&CPS Europe), 9th-12th June 2020, Madrid, Spain.
83. Sinha Ashish Kumar, Kumar Prashant, Prince and Hati, Ananda Shankar, "ANN Based Fault Detection Scheme for Bearing Condition Monitoring in SRIMs using FFT, DWT and Band-pass Filters" 2020 International Conference on Power, Instrumentation, Control, and Computing (PICC) 2020 IEEE.
84. Prince Kumar and Hati, Ananda Shankar, "Sensor-less Speed Control of Ventilation System Using Extended Kalman Filter For High Performance," 2021 IEEE 8th Uttar Pradesh Section International Conference on Electrical, Electronics and Computer Engineering (UPCON), 2021, pp. 1-6.
85. Kumar Prashant and Hati, Ananda Shankar "Support Vector Classifiers based broken rotor bar detection in Squirrel cage induction motor" Machines, Mechanisms and Robotics, Springer, Singapore, 429-438.
86. Hati, Ananda Shankar, and Chatterjee, T. K., "Some studies on condition monitoring techniques for online condition monitoring and fault diagnosis of mine winder motor", International Journal of Engineering Science and Technology (IJEST), vol. 4, no. 08, pp. 3785-3793, August 2012.
87. Hati, Ananda Shankar, and Chatterjee, T. K., "Axial leakage flux-based online condition monitoring instrumentation system for mine winder motor" Journal of Mines, Metals & Fuels, vol. 63, no. 5&6, pp. 132-140, May-June 2015.
88. Hati, Ananda Shankar, and Chatterjee, T. K., "Current monitoring Instrumentation system for detecting airgap eccentricity in mine winder motor", International Journal of Applied Engineering Research, vol. 10, no. 22, pp. 43000-43007, 2015.
89. Hati, Ananda Shankar, "Vibration monitoring instrumentation system for detecting airgap eccentricity in mine winder motor" Journal of Mine Metals and Fuels, vol. 64, no. 5&6, pp. 240-248, May-June 2016.
90. Magare, M. Lamin, and P. Chakrabarti, “Inherent Mapping Analysis of Agile Development Methodology through Design Thinking”,” Lecture Notes on Data Engineering and Communications Engineering, vol. 52, pp. 527–534, 2020
91. Kukreja P, Kukreja BJ, Qahtani NF, Qahtani MF, Qahtani MF, Qahtani AF. Awareness of Covid -19 among dental students: A preliminary study. Int J of applied dental sciences 2021; 7(1): 341-344
92. Kukreja BJ, Bhat KG, Kukreja P, Kumber VM, Balakrishnan R, Govila V. Isolation and immunohistochemical characterization of periodontal ligament stem cells: A preliminary study. J Indian Soc Periodontol 2021; 25: 295-9.
93. Kumar M, Goyal M, Jha B, Tomar S, Kushwah A. An Innovative procedure for lip lengthening in a patient with a short upper lip and high angle skeletal class II pattern: A case Report. J Ind orth soc 2021; 30: 1-8
94. Saleem R, Kukreja BJ, Goyal M, Kumar M. Treating short upper lip with “Unified lip repositioning” technique: Two case reports. J Indian Soc Periodontol 2022; 26: 89-93.
95. P Tyagi, VW Dodwad, S Vaish, T Chaudhary, N Gupta, Bhavna Jha Kukreja. Clinical efficacy of subgingivally delivered Punica Granatum chip and gel in management of chronic periodontitis patient. Kathmandu University Medical Journal. July 2020: 18(71); 279-83.
96. Kukreja P, Kukreja BJ, Ganesh R D’souza J, Abdelmagyd H, Recent advances in maxillofacial surgery – robotics and artificial intelligence. Harbin Gongye Daxue Xuebao/J Harbin Inst Technol. 2022; 9:95–98.
97. Gupta S, Rangappa KKG, Rani S, Ganesh R, Kukreja P, Kukreja BJ. Periodontal and Dentition

Status among Psychiatric Patients in Indore: A Descriptive Cross-sectional Study. J Contemp Dent Pract. 2022;23(12):1260–1266.
98. Kukreja BJ, Bhat KG, Kukreja P, Nayak A, Kotrashetty V, Dindawar S, et al. Regeneration of periodontal ligament fibers around mini dental implants and their attachment to the bone in an animal model: A radiographic and histological study. J Indian Soc Periodontol. 2023; 27:167-73
99. Talib YM, Albalushi WN, Fouad MD, Salloum AM, Kukreja BJ, H Abdelmagyd. Bilateral Inverted and Impacted Mandibular Third Molars: A Rare Case Report Third Molars: A Rare Case Report, Cureus. 2023: 2-9
100. Kukreja P, Kukreja BJ, Bhat KG.Detection and Quantification of Treponema denticola in Subgingival Plaque of Humans by Polymerase Chain Reaction. Bangladesh J Medical Sci. 2023;22 Special Issue:93-99
101. Katariya A, Kukreja BJ, Dinda S.C,Singh S, Bhat KG. A microbiological study to evaluate the effect of different concentrations of coenzyme q10 in inhibiting key pathogens of periodontitis. Eur. Chem. Bull. 2023,12(10), 5826-5843
102. Zannah, S. Rachakonda, A. M. Abubakar, S. Devkota, and E. C. Nneka, "Control for Hydrogen Recovery in Pressuring Swing Adsorption System Modeling," FMDB Transactions on Sustainable Energy Sequence, vol. 1, no. 1, pp. 1–10, 2023.
103. Y. Abdullahi, A. Bhardwaj, J. Rahila, P. Anand, and K. Kandepu, "Development of Automatic Change-Over with Auto-Start Timer and Artificial Intelligent Generator," FMDB Transactions on Sustainable Energy Sequence, vol. 1, no. 1, pp. 11–26, 2023
104. V. K. Nomula, R. Steffi, and T. Shynu, "Examining the Far-Reaching Consequences of Advancing Trends in Electrical, Electronics, and Communications Technologies in Diverse Sectors," FMDB Transactions on Sustainable Energy Sequence, vol. 1, no. 1, pp. 27–37, 2023.
105. M. Siddique, Z. M. Sarkinbaka, A. Z. Abdul, M. Asif, and N. Elboughdiri, "Municipal Solid Waste to Energy Strategies in Pakistan And Its Air Pollution Impacts on The Environment, Landfill Leachates: A Review," FMDB Transactions on Sustainable Energy Sequence, vol. 1, no. 1, pp. 38–48, 2023.
106. B. Senapati, R. Regin, S. S. Rajest, P. Paramasivan, and A. J. Obaid, "Quantum Dot Solar Cells and Their Role in Revolutionizing Electrical Energy Conversion Efficiency," FMDB Transactions on Sustainable Energy Sequence, vol. 1, no. 1, pp. 49–59, 2023.
107. G. Mehta, S. Rubin Bose, and R. Selva Naveen, "Optimizing Lithium-ion Battery Controller Design for Electric Vehicles: A Comprehensive Study," FMDB Transactions on Sustainable Energy Sequence, vol. 1, no. 2, pp. 60–70, 2023.
108. Nwabuokei, M. Ghouse, W. Chen, E. T. Raphael Kollannur, H. Li, and R. Bin Sulaiman, "Quantifying the Influence of Population on Carbon Emissions: A Comparative Study of Developed versus Developing Countries Using Machine Learning," FMDB Transactions on Sustainable Energy Sequence, vol. 1, no. 2, pp. 71–82, 2023.
A. Victor Ikwuagwu, N. Henry Ononiwu, and K. Adeyemi, "Comprehensive Energy Analysis and Performance Evaluation of Lithium-Ion Battery Integration in Photovoltaic Systems: A Comparative Study on Reliability and Environmental Impact," FMDB Transactions on Sustainable Energy Sequence, vol. 1, no. 2, pp. 83–93, 2023.
109. R. Raj Saxena, R. Saxena, and A. Patel, "Functional Electrical Stimulation as a Significant Bioelectronic Intervention in the Domain of Fitness: A Review," FMDB Transactions on Sustainable Energy Sequence, vol. 1, no. 2, pp. 94–106, 2023.
110. L.N. Ramya, S. Rubin Bose, R. Selva Naveen, and R. Islam Chowdhury, "Advanced Solar Charge Controller: Integrating MPPT Technology and Online Data Logging for Efficient Energy Management," FMDB Transactions on Sustainable Energy Sequence, vol. 1, no. 2, pp. 107–120, 2023.